Progress in Nuclear Energy 63 (2013) 86–95

Contents lists available at SciVerse ScienceDirect

Progress in Nuclear Energy

journal homepage: www.elsevier.com/locate/pnucene

Conceptual design of a supercritical water reactor with double-row-rod assembly

Chuanqi Zhao [a], Liangzhi Cao [a,*], Hongchun Wu [a], Jue Yang [b], Yong Zhang [b]

[a] School of Nuclear Science and Technology, Xi'an JiaoTong University, Xi'an Shaanxi 710049, China
[b] China Nuclear Power Technology Research Institute, Guangdong Shenzhen 518026, China

ARTICLE INFO

Article history:
Received 13 May 2012
Received in revised form
2 November 2012
Accepted 8 November 2012

Keywords:
SCWR
Double-row-rod assembly
Three-dimensional N/TH coupling

ABSTRACT

A novel type of fuel assemblies with double rows of fuel rods between water rods is proposed and optimized for a supercritical light water reactor design. It brings improved neutron moderation and lower local power peak. Gadolinium is introduced as burnable poison to reduce excess reactivity at the beginning of the fuel cycle. The optimizations for the fuel rods with gadolinium are performed in the present paper. SS316L is used for fuel rod cladding and structural material. In order to reduce the amount of SS316L because of its high thermal neutron absorption, honeycomb structure filled with thermal isolation is introduced to replace the solid stainless steel. The two-pass water flow scheme is chosen with more fuel assemblies for downward flow. Fuel in-core loading pattern and control rod clusters pattern are designed to flatten power distribution at inner regions to enhance coolant outlet temperature. Axial fuel enrichment is zoned into three regions to control axial power peak, which might affect maximum cladding surface temperature. An equilibrium core is then analyzed based on neutronics/thermal-hydraulics coupling model. The numerical results indicate that a high average coolant outlet temperature of 500 °C is achieved with a maximum cladding surface temperature less than 650 °C. The void reactivity effects of moderator and coolant are negative throughout the cycle.

© 2012 Elsevier Ltd. All rights reserved.

1. Introduction

Supercritical light water reactor (SCWR) is a thermal reactor cooled and moderated by supercritical water. Water does not exhibit a phase change from liquid to gas above 22.1 MPa. Therefore, the plant system is simpler and more compact than PWRs and BWRs without a dryer, water-steam separators and recirculation pumps. The coolant outlet temperature is high because there is no limitation of saturation temperature at supercritical pressure. This results in high thermal efficiency, which is good not only for producing electricity but also for reducing the amount of spent fuel per generated watt of electricity.

As supercritical water doesn't undergo a change of phase, the Maximum Cladding Surface Temperature (MCST) is taken as design criterion for SCWR. Average coolant outlet temperature is also an important parameter, because it directly affects the thermal efficiency. The closed channel is designed to avoid coolant mixing between fuel assemblies. Thus, a uniform power distribution within an assembly is very important for increasing the outlet temperature while keeping a low MCST. This is paid attention to in previous studies, but there is still room for improvements. In SCWR of Japan (JSCWR) (Yamaji et al., 2005a, 2005b; Kamei et al., 2006), assemblies with single row of fuel rods between water rods are used in core design. Fuel rods in the periphery of the assembly and the corner of water rods have lower power than others. In order to provide uniform neutron moderation, peripheral water rods are used which increase the complexity of the assembly. Another promising design is the European High Performance Light Water Reactor (HPLWR) (Schulenberg et al., 2011; Maráczy et al., 2011). A small, square, 7 by 7 fuel pin lattices with a water rod occupying 9 lattices in the center has been designed for the HPLWR fuel assembly. An assembly cluster consists of 3 by 3 assemblies. There is gap between assemblies filled with moderator. In this assembly, 4 corner pins have better moderation than the remaining ones. Thus, two different enrichments are used to flatten local radial power distribution, which makes the assembly complex. In this study, assemblies with dual rows of fuel rods between water rods is chosen, which results in improved uniformity of neutron moderation and coolant temperature (Liu and Cheng, 2010a). This assembly has been used in a mixed spectrum core (Liu and Cheng, 2010b, 2010c). However, some optimizations should be made to satisfy the thermal core. The thickness of water rods wall and assembly box is larger than that of assemblies in previous studies (Yamaji et al., 2005a, 2005b; Kamei et al., 2006) for engineering

* Corresponding author. Tel.: +86 29 8266 3285; fax: +86 29 8266 7802.
E-mail address: caolz@mail.xjtu.edu.cn (L. Cao).

0149-1970/$ – see front matter © 2012 Elsevier Ltd. All rights reserved.
http://dx.doi.org/10.1016/j.pnucene.2012.11.002

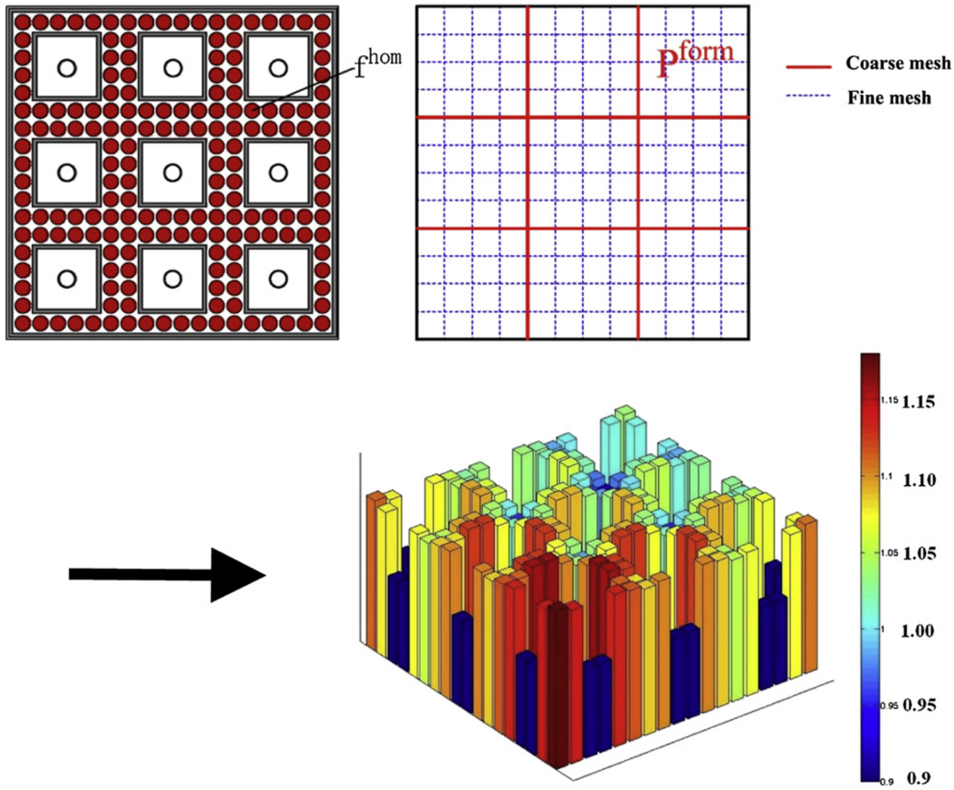

Fig. 1. Assembly power reconstruction.

feasibility, which causes higher fuel enrichment. Burnable poison is introduced to reduce the excess reactivity.

Based on this assembly, a core is designed and analyzed using coupling model of three-dimensional neutronic and thermal-hydraulic. With assembly power reconstruction, pin power distribution is obtained to improve the accuracy of coupling calculation.

This paper is organized as follows. Section 2 introduces the methods used in assembly and core design. Section 3 performs some optimizations on fuel assembly design. Section 4 studies the

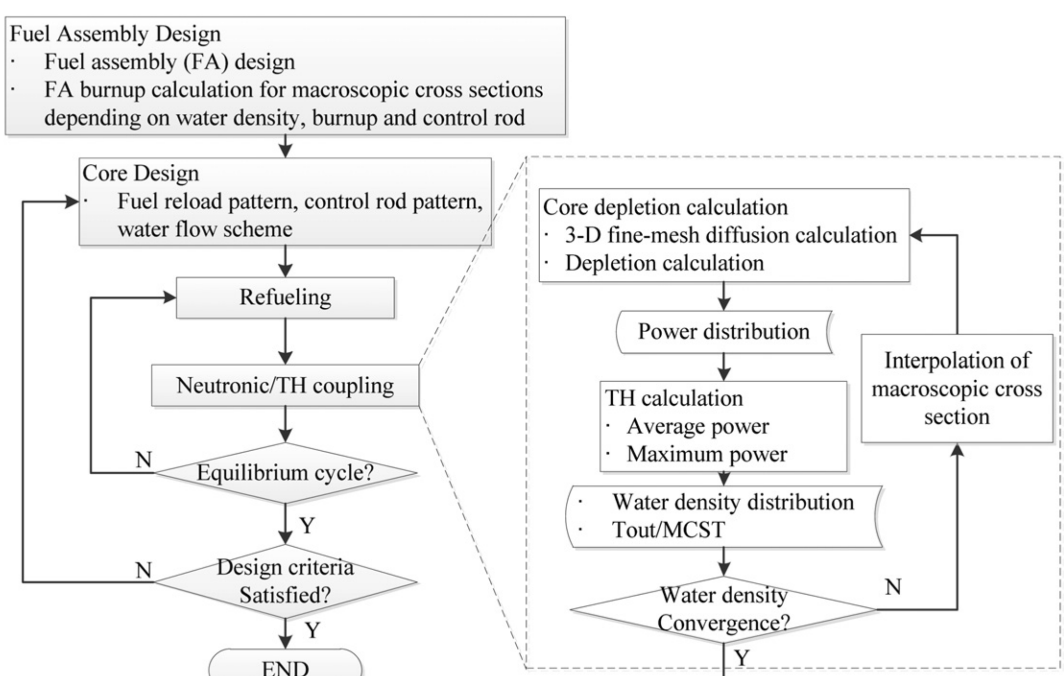

Fig. 2. Equilibrium core design method.

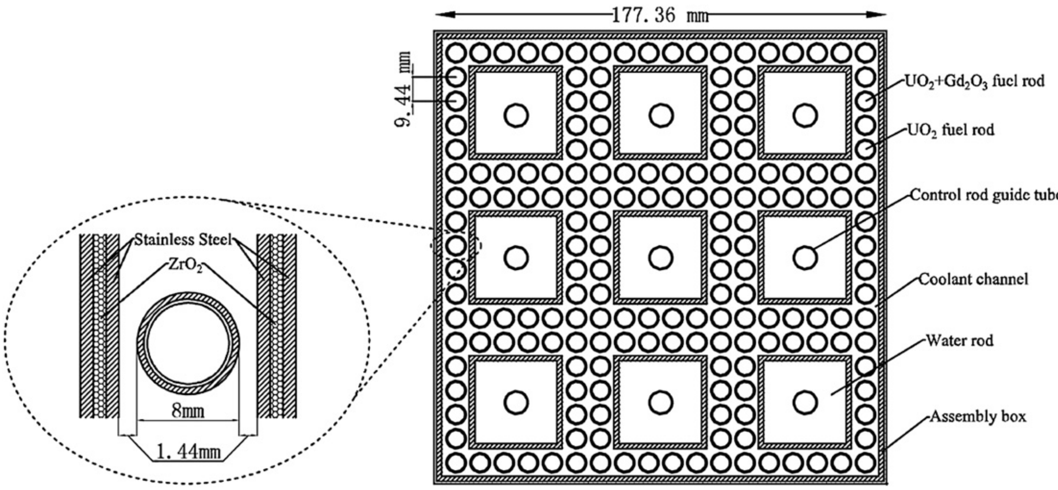

Fig. 3. Fuel assembly horizontal cross section.

core design. Finally, some results and conclusions are summarized in Sections 5 and 6.

2. Core design method

2.1. Neutronic calculations

The DRAGON code (Marleau et al., 2010) based on collision probability techniques is used to perform the two-dimensional assembly transport calculation for lattice physics study and generate the macroscopic cross sections and diffusion coefficients for subsequent core calculations. Cross sections are taken from the 69-group WIMS-D library based on ENDF/B-VII data. Two-dimensional fuel assembly burnup calculations are carried out with water densities expected in the equilibrium core. At the end of burnup calculation, the energy groups are collapsed to four energy groups (2 fast and 2 thermal), and assembly homogenized macroscopic cross sections are obtained as a function of water density and burnup. All of these cross sections are prepared for two cases, with or without control rods.

Core depletion calculation is based on three-dimensional multi-group diffusion code CITATION (Fowler and Vondy, 1971). As CITATION has no function of depletion calculation, an auxiliary code has been developed (Yang et al., 2011). The calculation is carried out in quarter core symmetry using four energy groups, which correspond to the four collapsed energy groups obtained by the fuel assembly burnup calculations. In order to improve the calculation accuracy, a tight mesh size with radial size of 1.5 cm by 1.5 cm and axial size of 3.0 cm is chosen.

2.2. Assembly power reconstruction

After assembly depletion calculations mentioned above, the fuel rod power distribution in an assembly is obtained and made into an interpolation table of water density, burnup and control rods. Ratio of fuel rod power to average assembly power (f^{hom}, form factor) for fuel rod α, for example, could be interpolated from the table with core operating conditions. In core depletion calculations, the fuel assemblies are divided into fine meshes in X, Y and Z directions, and power of each fine mesh is obtained. Based on the fine mesh power, the power of nine coarse meshes corresponding to nine subassemblies (one water rod and one row of surrounding fuel rods) could be achieved. The fine mesh power distribution is affected by the position of the fuel assembly in the core. Thus the power of coarse mesh is also a function of fuel assembly position. The power of mesh A, which fuel rod α belongs to, is P^{form}. Then, the reconstruction power of fuel rod α could be obtained (see Fig. 1):

$$P = P^{\mathrm{form}} f^{\mathrm{hom}} \tag{1}$$

2.3. Thermal hydraulic calculations

The thermal hydraulic calculations are carried out using in-house code based on single-channel model. Each fuel assembly in the core is treated as one channel. The single-channel calculation is carried out with two kinds of power: one is average power of the assembly for getting coolant and moderator density distribution and the other is maximum fuel rod power for getting maximum cladding surface temperature (MCST). Heat transfer coefficients are determined by the Oka–Koshizuka correlation (Oka et al., 2011). With the spatial power distribution calculated by core depletion calculation and assembly power reconstruction, average and maximum power of each assembly can be obtained at all burnup steps. Considering maximum power of each assembly through the whole cycle, the core coolant flow rate distribution can be searched to satisfy the MCST limitation. With the flow rate distribution, water density distributions at all burnup steps could be calculated using average power of each assembly. Both co-current flow mode and counter-current flow mode are considered to model water flow scheme in peripheral and inner fuel assembly, respectively. With pin power distribution, sub-channel analysis could be carried out using ATHAS (Li et al., 2009; Shan et al., 2009) in future studies.

2.4. Equilibrium core design method

The equilibrium core design method is shown in Fig. 2. The equilibrium core, in this study, is defined such that the burnup distribution and water density distribution at the beginning of (n)th cycle (BOC) are identical to those at the beginning of (n+1)th cycle

Table 1
Power peaking factors of different gap sizes.

Gap width (mm)	Radial power peaking factor
1.44	1.085
1.00	1.091
0.72	1.094
0.50	1.097

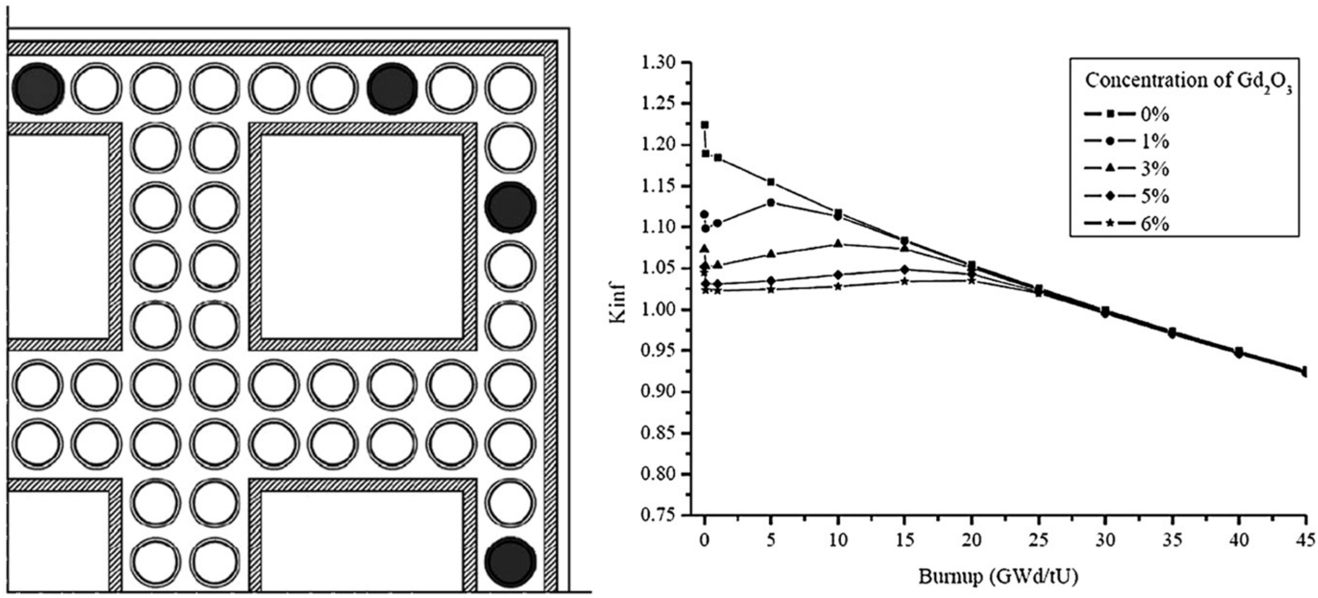

Fig. 4. Scheme 1 of poison rods position and results of different concentrations.

of operation. After all core design parameters are determined, the first cycle is calculated with neutronic and Thermal-hydraulic coupling until water density distributions are converged. In order to simplify calculations, coupling calculations are performed through the cycle. Then, according to fuel reload pattern, burnup distribution of the second cycle is obtained. The core calculations for one cycle of operation, followed by the replacement of fuel assemblies, are repeated until the BOC burnup distribution is converged. When the BOC burnup distribution is converged, the equilibrium core is reached by definition.

3. Fuel assembly design

The horizontal cross section of a fuel assembly is shown in Fig. 3. The fuel assembly consists of 180 fuel rods, 9 square water rods. The outer diameter of fuel rods is 8.0 mm and fuel rod pitch is 9.44 mm. These dimensions are chosen to achieve a higher heat transfer capability. The thickness of stainless steel cladding (SS316L) is 0.5 mm taking buckling collapse, stress rupture and creep rupture at both normal operation and abnormal transient conditions into account.

From the viewpoint of engineering feasibility, thickness of water rods wall and assembly box is determined to be 2 mm. The material is SS316L. Stainless steel has a large neutron absorption cross section, which leads to high fuel enrichment. Honeycomb structures could reduce the usage of stainless steel with a similar stiffness (Herbell et al., 2008). The box walls of water rods and assembly are built as a stainless steel sandwich construction with an internal honeycomb cells. The honeycomb cells are filled with ZrO_2 for thermal isolation. Moreover, with the thermal isolation,

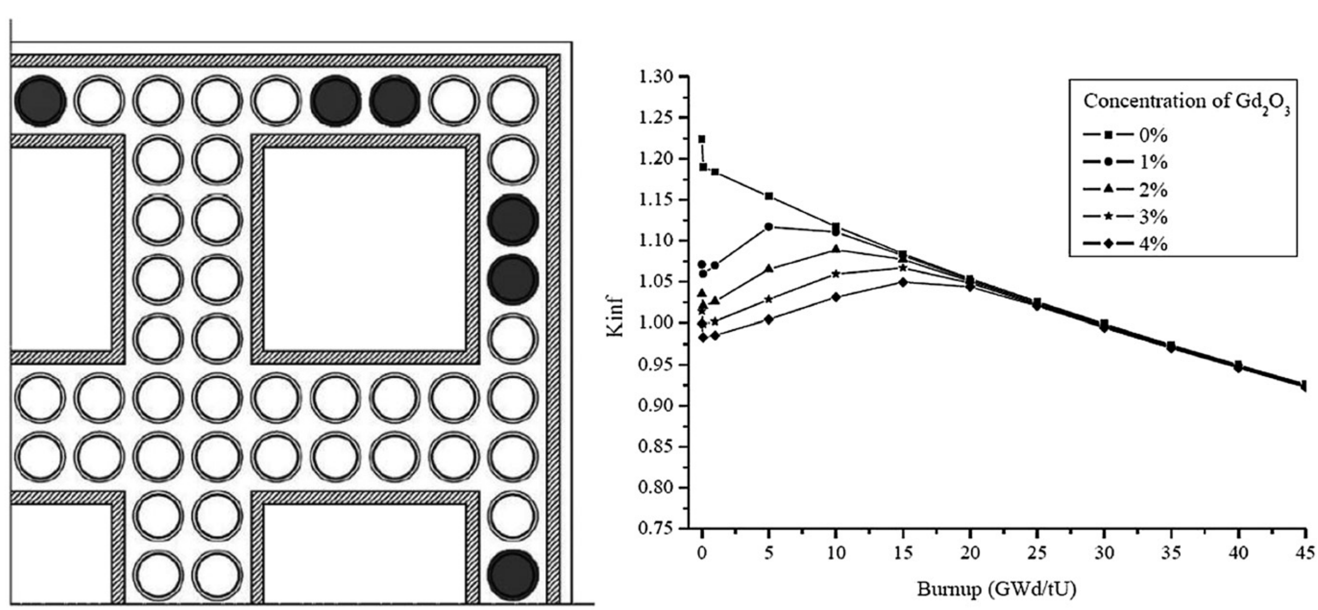

Fig. 5. Scheme 2 of poison rods position and results of different concentrations.

Table 2
Radial power peaking factors of different cases.

No. of poison rods	Concentration (wt%)	Radial power peaking factor
0	0	1.085
4	1	1.085
	3	1.090
	5	1.094
	6	1.096
6	1	1.087
	2	1.096
	3	1.102
	4	1.109

temperature of moderator in water rods is kept under pseudo critical temperature, which is beneficial to neutron moderation.

There is a gap between fuel assemblies for mechanical behavior. Water in the gap is taken as moderator, which on one hand enhances neutron moderation for peripheral fuel rods, on the other hand causes higher local peaking factor. Considering both effects, the width of gap between assemblies is determined to be 2 mm. Gaps between fuel rods and water rods wall, fuel rods and the assembly box are crucial to local peaking. Thus an analysis is done on the gap width (average condition, coolant density at 0.2 g/cc, moderator density at 0.6 g/cc). The main results are given in Table 1. The results show that the local power peaking factor increases as the gap width decreases. This is understandable because neutron moderation is less uniform as fuel rods are closer to water rods. From this point, 1.44 mm is chosen as gap width.

For the burnup reactivity compensation, burnable poison (Gd_2O_3) is mixed with the fuel. Meanwhile, burnable poison decreases excess reactivity at the BOC and thus the number of control rods could be reduced. However, the number and position of fuel rods mixed with Gd_2O_3 and the concentration of Gd_2O_3 need to be optimized. Two alternative schemes of the position of burnable poison rods are chosen, according to radial power distribution obtained in assemblies without burnable poison. Cases of different concentrations of Gd_2O_3 are calculated based on these two schemes. The brief results are shown in Figs. 4 and 5 and Table 2. The optimization principles are as follows: first, the infinite multiplication factor should be close to 1.0 to reduce the number of control rods; second, the radial power peaking factor should be under 1.10 to achieve uniform coolant temperature distribution; last, the burnable poison should be consumed at the end of first cycle (around 15 GWd/t) to minimize fuel enrichment. According to these principles, the position shown in Fig. 5 is taken and the concentration is 2.0 wt%.

All water rods are equipped with control rod guide tubes, which allow a cluster-type control rod unit (natural B_4C) to be inserted from the top of the core. Relevant dimensions of control rods are the same as fuel rods.

4. Core design

4.1. Design summary

The core is operating at the pressure of 25 MPa. The average inlet and outlet temperature are 280 °C and 500 °C respectively. The thermal efficiency is 43.8%, according to the relationship between coolant outlet temperature and thermal efficiency given in a previous study (Dobashi et al., 1997). The target electric power scale is 1000 MWe, thus the power scale corresponds to a thermal output of about 2280 MWt. The core size is determined based on three points: First, the level of the core power density is expected to be similar to current LWRs (from about 50W/cm^3 for BWRs to about 100W/cm^3 for PWRs). Second, it's easier to flatten the radial power distribution with more fuel assemblies, but the replacement work will be more complex. Third, the core is a three-batch core with one fourth cycle fuel assembly loaded at the center and the core is quadrant symmetric, therefore, the number of fuel assemblies should be given by $12N + 1$. Thus, the number of fuel assemblies is 241; the active core height is 4.2 m; the average linear heat generation rate (ALHGR) is 12.5 kW/m, which means the power density is 71.6 W/cm^3. The initial fuel inventory of the core is 58.8 t, less than that of current PWRs.

The following principles are considered to ensure fuel and core safety:

- Positive water density reactivity effect (negative void reactivity effect)
- Maximum cladding surface temperature (MCST) less than or equal to 650 °C
- Maximum linear heat generation rate (MLHGR) less than or equal to 39.0 kW/m
- Core shutdown margin greater than or equal to 1.0% dk/k

The MCST is determined to ensure fuel integrity at both normal operation and abnormal transients. The MLHGR criterion is necessary for fuel centerline temperature limitation. Besides these criteria, moderator temperature should be less than the pseudo critical temperature at 25 MPa (384 °C) to provide sufficient neutron moderation.

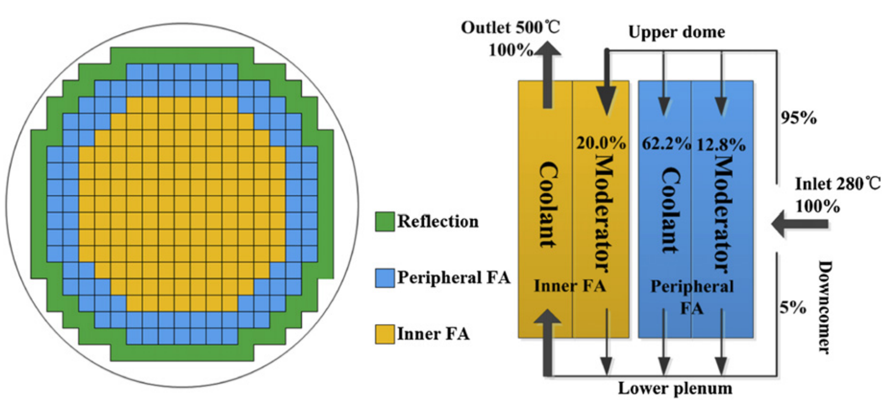

Fig. 6. Core horizontal cross section and water flow scheme.

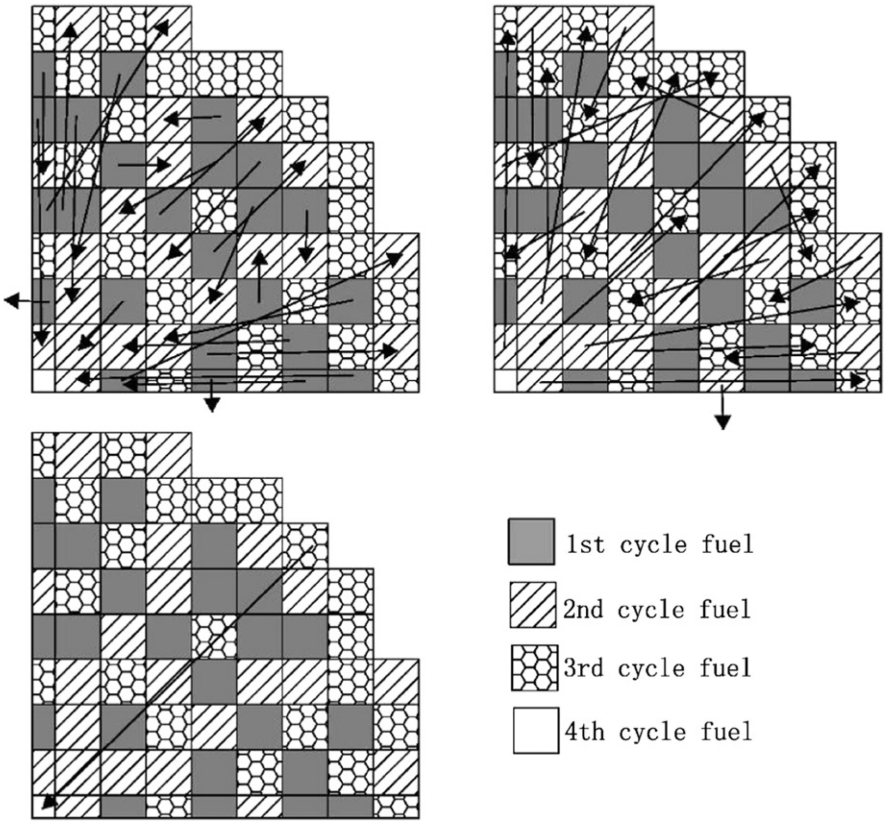

Fig. 7. Fuel loading pattern (quarter symmetric core).

4.2. Water flow scheme

As illustrated in Fig. 6, 95% of the feed water is led to upper dome and the rest flows down through downcomer. Most of water in the upper dome is distributed to fuel channel as coolant in peripheral fuel assemblies, and it flows down through the core. All of the feed water mixes uniformly at the lower plenum and rises upward through coolant channel of inner fuel assemblies to outlet.

The number of peripheral fuel assemblies is more than that of previous studies. It leads to higher coolant velocity in inner fuel assemblies, which enhances heat transfer coefficient. The power generation is lower in peripheral fuel assemblies than that in inner fuel assemblies. This flow scheme could flatten outlet temperature for all outlet coolant heated in inner fuel assemblies. Besides, the higher average water density of peripheral fuel assemblies could increase power generation of peripheral fuel assemblies and flatten the radial power distribution.

4.3. Fuel loading pattern

The fuel loading pattern and shuffling scheme for a quarter symmetric core are shown in Fig. 7. The low leakage fuel loading pattern is used to reduce fuel enrichment. Most peripheral fuel assemblies have stayed in the core for one or two cycles. Fresh fuel assemblies are then check-boarded with other 2nd and 3rd cycle fuel assemblies in the interior of the core to flatten radial power distribution.

4.4. Axial fuel enrichment distribution

Axial fuel enrichment was set to be uniform at the beginning. Calculations showed that peak of axial power distribution of the BOC appeared at the bottom and moved upward to the top as burnup increases. Axial power peaking factor reached nearly 2.0 at the BOC and EOC, which caused high MCST. In order to flatten axial power distribution, fuel assembly is axially divided into three partitions with different enrichments. As shown in Fig. 8, enrichments of top, middle and bottom parts are 6.4 wt%, 6.8 wt% and 6.4 wt%, respectively. The average enrichment is 6.60 wt%, higher than that of previous studies (Yamaji et al., 2005a, 2005b; Kamei et al., 2006). As mentioned above, this is caused by more usage of

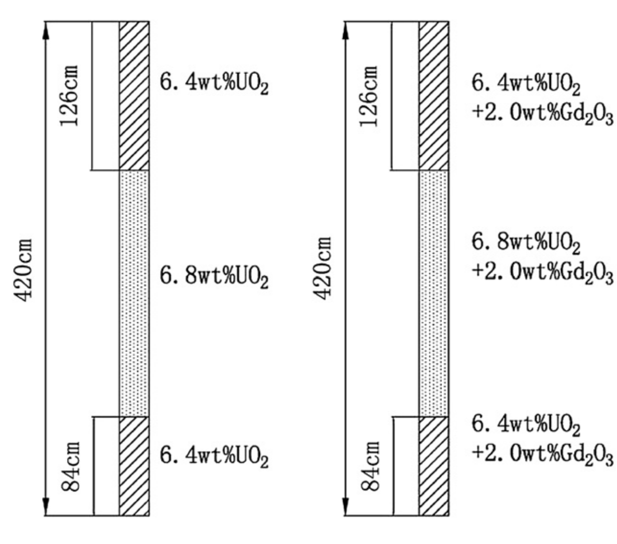

Fig. 8. Axial fuel enrichment distribution.

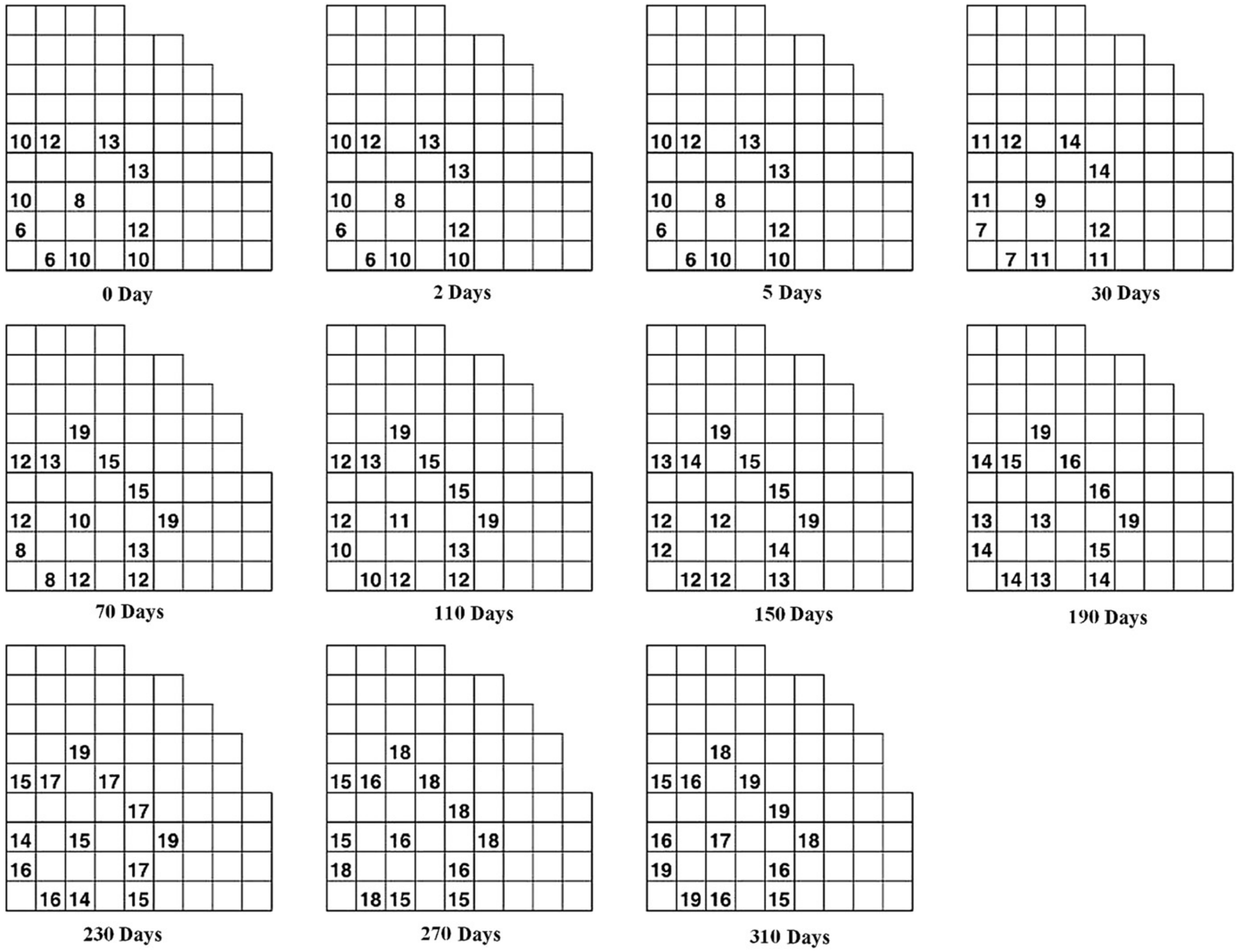

Fig. 9. Control rod pattern (quarter symmetric core).

stainless steel and less fuel inventory. Concentration of Gd_2O_3 is 2.0 wt% for all three parts.

4.5. Control rod pattern

Control rod pattern is shown in Fig. 9. Each box represents a fuel assembly and the number in it represents number of meshes between control rod end and the bottom of the core. Zero means a completely inserted rod while twenty (the blank box) indicates a completely withdrawn rod.

Table 3
Primary core characteristics.

Operation pressure (MPa)	25
Thermal/electrical power (MW)	2280/1000
Cycle length (EFPD)	310
Equivalent diameter/active length (m)	3.14/4.2
Average outlet temperature (°C)	500
Mass flow rate (kg/s)	1181
Fuel enrichment bottom/mid/top/average (wt%)	6.4/6.8/6.4/6.6
Fuel assembly average discharge burnup (GWd/t)	40.0
Maximum discharge burnup (GWd/t)	51.6
MLHGR/ALHGR (kW/m)	35.2/12.5
Average power density (W/cm^3)	71.6
MCST (°C)	641

−1.00	−1.00	−1.00	−1.00					
−1.00	−1.00	−1.00	−1.00	−1.00	−1.00			
1.02	1.02	0.88	0.88	−1.00	−1.00	−1.00		
0.94	0.90	1.06	0.98	1.05	−1.00	−1.00	−1.00	
1.01	1.03	1.02	1.06	0.93	1.05	−1.00	−1.00	
1.01	1.04	0.99	1.01	1.06	0.98	0.88	−1.00	−1.00
1.06	1.04	1.03	0.99	1.02	1.06	0.88	−1.00	−1.00
1.00	1.04	1.04	1.04	1.03	0.90	1.01	−1.00	−1.00
0.97	1.00	1.06	1.01	1.01	0.94	1.02	−1.00	−1.00

Fig. 10. Coolant flow rate distribution (quarter symmetric core).

The control rod pattern is determined to control excess reactivity as well as to keep the balance of radial and axial power distributions. Some control rods remain inserted at the EOC to prevent power peak near the top, which could cause a high cladding surface temperature.

5. Results of equilibrium core

Primary system parameters of the equilibrium core are shown in Table 3.

5.1. Coolant flow rate distribution

As mentioned above in Section 2.3, the moderator flow rate of peripheral assemblies is equal to each other, so is the coolant flow rate of peripheral assemblies and the moderator flow rate of inner assemblies (see Fig. 6). The ascending coolant flow rate distribution in inner fuel assemblies is searched through the cycle to satisfy the MCST criterion. For each assembly, maximum of flow rate at all burnup steps is chosen. The coolant flow rate distribution is illustrated in Fig. 10. The white and shaded boxes represent inner and peripheral fuel assemblies, respectively. The values in white boxes denote the ratio of the coolant flow rate in this fuel assembly relative to the average flow rate of ascending coolant in inner fuel assemblies. −1.00 in shaded boxes means that the coolant flow rate in each shaded box is the same and the coolant flows downwards.

5.2. Power distribution, peaking factors and MLHGR

Axially averaged radial power distribution for a quarter symmetric core at the BOC, middle of a cycle (MOC) and EOC are shown in Fig. 11. The radial power peaking factors at the BOC, MOC and EOC are 1.378, 1.264 and 1.282, respectively. This is a little larger but the radial power peaking factors of inner FAs are lower, which at the BOC, MOC and EOC are 1.16, 1.09 and 1.11, respectively. This leads to more uniform coolant outlet temperatures.

The horizontally averaged axial power distribution at the BOC, MOC and EOC are shown in Fig. 12. Power peak shifts from the bottom to top as the burnup increases and the control rods are gradually withdrawn. The axial power peaking factors are kept lower than 1.6 through the cycle.

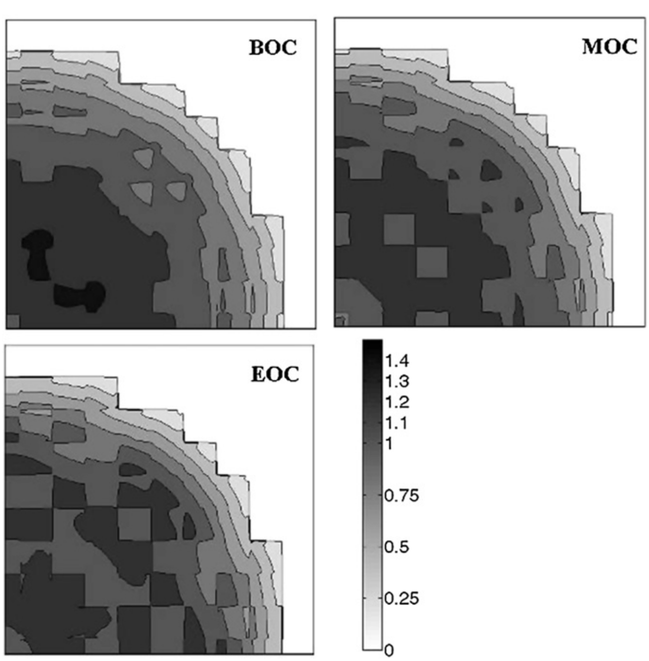

Fig. 11. Radial power distribution (quarter symmetric core).

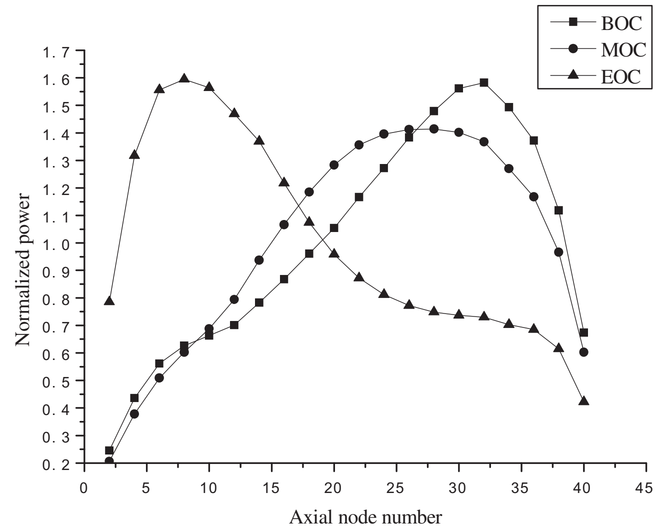

Fig. 12. Axial power distribution.

Since assembly power reconstructions are done, MLHGR could be evaluated more accurately than previous studies. The result shows that MLHGR through operation cycle is 35.2 kW/m. The calculated MLHGR is less than the criterion value, but the uncertainties are not yet taken into account. The current 3.8 kW/m distance to criterion value is not enough to cover uncertainties and maneuvering range, but with further optimization of axial and radial power distribution, it could be improved.

At the end of equilibrium cycle, the axially averaged radial burnup distribution is given in Fig. 13. The maximum discharge burnup is 51.6 GWd/t and the average burnup is 40 GWd/t.

5.3. Coolant temperature and MCST distributions

The coolant outlet temperature and MCST distributions at the BOC, MOC and EOC for a quarter symmetric core are shown in

37.7	24.1	37.8	21.5					
13.4	41.5	12.3	37.4	39.0	34.7			
14.8	14.5	35.1	26.7	13.5	27.0	37.4		
29.2	39.2	15.8	30.9	14.6	14.5	27.0	36.5	
15.8	16.1	31.0	16.0	46.2	14.6	13.5	39.1	
46.4	29.0	42.5	30.9	16.0	30.9	26.7	37.4	21.6
15.9	30.9	15.9	42.5	31.0	15.8	35.2	12.3	37.8
30.0	31.8	30.9	29.0	16.1	39.3	14.5	41.5	24.1
51.6	30.0	15.9	46.4	15.8	29.3	14.8	13.4	37.8

Fig. 13. Burnup distribution at the EOC (GWd/t).

BOC
MOC
EOC

463 495 513	462 489 505	484 492 492	484 492 486					
531 535 522	520 521 515	486 507 506	497 504 503	450 482 503				
510 523 513	513 522 514	532 518 504	493 511 525	474 488 505	450 482 503			
513 486 474	547 520 500	536 506 488	541 523 509	491 509 522	497 504 503	484 492 486		
519 506 510	547 508 504	523 517 525	536 506 488	532 519 504	486 507 506	482 491 491		
524 487 516	533 491 506	547 508 504	547 520 500	513 523 513	519 522 514	462 490 505		
507 461 475	524 487 516	519 506 510	513 486 474	510 523 513	531 535 522	463 495 513		

Fig. 14. Coolant outlet temperature distributions (quarter symmetric core, °C).

Figs. 14 and 15. In Figs. 14 and 15, shaded boxes stand for peripheral FAs, where the coolant drifts to the lower plenum and the MCST is relatively low. Average coolant outlet temperature is 500 °C. The coolant outlet temperature for ascending flow varies from 450 to 547 °C. It is more uniform because of lower radial power peaking factor of inner FAs. The MCST through the cycle is 641 °C, which is below the design criterion. However, the engineering uncertainties have not been considered yet. The MCST appears at the EOC because of axial power peak near the top of the core.

5.4. Void reactivity effects and cold shutdown margin

For the fuel assembly, the void reactivity effects are calculated in two cases. Case 1: Keep the moderator density constant, the coolant density changes with the void fraction. Case 2: Keep the coolant

BOC
MOC
EOC

544 577 640	543 576 640	573 594 638	576 602 640					
611 616 629	616 604 628	577 585 640	599 598 640	531 563 640				
626 612 601	627 605 605	627 590 619	607 597 640	560 563 641	531 563 640			
626 566 581	626 591 602	626 570 586	627 599 634	603 593 640	599 599 640	576 604 640		
627 582 605	627 575 611	624 586 639	626 570 585	627 590 619	577 586 640	570 593 636		
625 566 640	627 563 617	627 575 611	626 592 602	627 606 605	615 605 627	544 578 640		
613 550 640	625 566 640	627 582 605	626 566 581	626 612 601	611 616 629	544 577 640		

Fig. 15. MCST distributions (quarter symmetric core, °C).

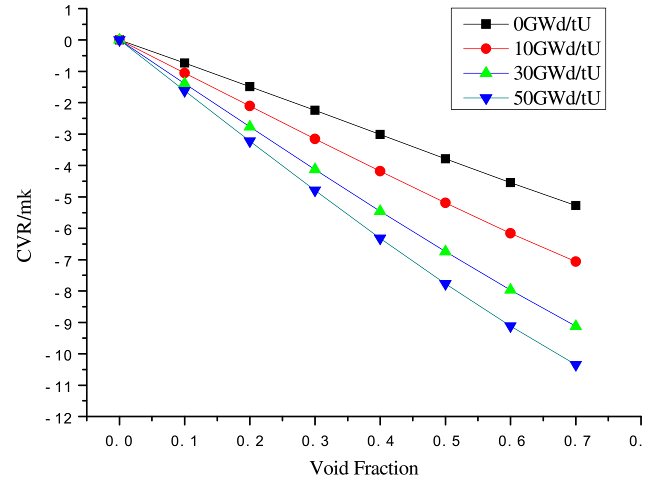

Fig. 16. Coolant void reactivity effect.

density constant, the moderator density changes with the void fraction. By increasing void fraction, void reactivity effects of coolant and moderator, in units of mk (1 mk = 100 pcm), could be evaluated and the results are shown in Figs. 16 and 17. They decrease as void fraction and burnup are increased, and keep negative. Moderator void reactivity effect is larger and changes faster than that of coolant because moderator is more significant in neutron moderation.

The void reactivity effect for the equilibrium core is also evaluated by assuming the feed water lost. The effects at BOC and EOC are −2.13% dk/k and −2.87% dk/k, respectively. The design criterion of negative void reactivity effects is satisfied as well.

The cold shutdown margin is evaluated for BOC at cycle burnup 0.0 GWd/t. In the evaluation, all water density is 1.0 g/cc and the insertion of the maximum worth control rod cluster is assumed to be failed. In order to provide sufficient negative reactivity, four banks of shutdown rods are introduced. The position of shutdown rods and the maximum worth control rod is shown in Fig. 18. The calculation is done for 1/2-symmetric core geometry. The effective multiplication factor of the core is evaluated to be 0.988. Thus the cold shutdown margin is 1.2% dk/k.

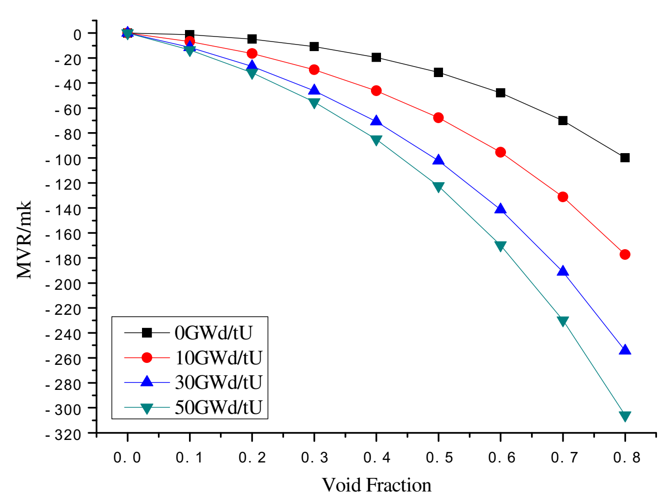

Fig. 17. Moderator void reactivity effect.

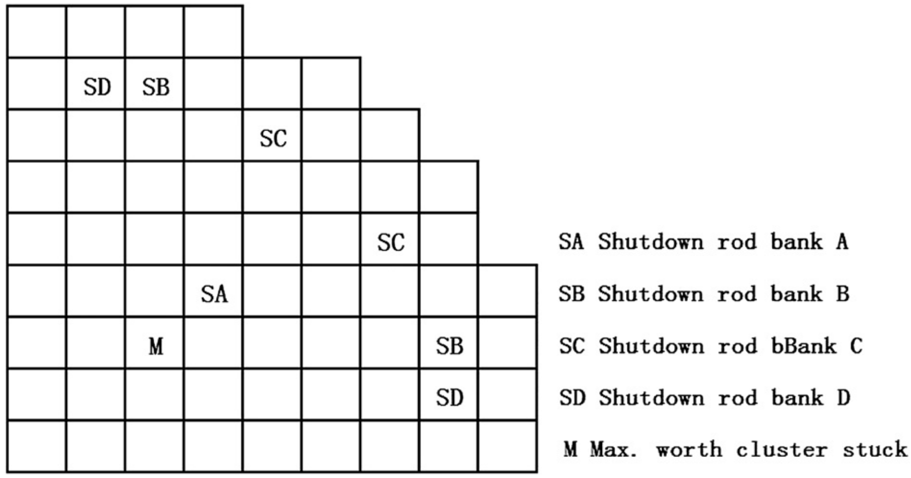

Fig. 18. Position of shutdown rods.

6. Conclusions

Fuel assemblies with double rows of fuel rods between water rods are used and optimized to get more uniform power distribution, considering engineering feasibility. An equilibrium core is designed and calculated with three-dimensional neutronic and thermal-hydraulic coupling. Assembly power reconstruction is carried out to get accurate power distribution, coolant temperature distribution and MCST. The result shows that this design is feasible and satisfies all given design criteria. However, further optimization of fuel assemblies based on sub-channel analysis should be done to minimize uranium enrichment. The uncertainties analysis should also be carried out in the future.

Acknowledgments

This work is financially supported by the National Science Foundation of China (Approved number 10976021) and the National Magnetic Confinement Fusion Science Program (Approved number 2010GB111007).

References

Dobashi, K., Oka, Y., Koshizuka, S., 1997. Core and plant design of the power reactor cooled and moderated by supercritical light water with single tube water rods. Annals of Nuclear Energy 24, 1281–1300.

Fowler, T.B., Vondy, D.R., 1971. Nuclear Reactor Core Analysis Code CITATION. ORNL-TM-2496. Oak Ridge National Laboratory.

Herbell, H., Himmel, S., Schulenberg, T., 2008. Mechanical analysis of an assembly box with honeycomb structure designed for a high performance light water reactor. In: International Students Workshop on High Performance Light Water Reactors, March 31 to April 3, Karlsruhe, Germany.

Kamei, K., Yamaji, A., Ishiwatari, Y., et al., 2006. Fuel and core design of super light water reactor with low leakage fuel loading pattern. Journal of Nuclear Science and Technology 43 (2), 129–139.

Li, C.Y., Shan, J.Q., Leung, L.K.H., 2009. Subchannel analysis of CANDU-SCWR fuel. Progress in Nuclear Energy 51, 799–804.

Liu, X.J., Cheng, X., 2010a. Thermal-hydraulic and neutron-physical characteristics of a new SCWR fuel assembly. Annals of Nuclear Energy 36, 28–36.

Liu, X.J., Cheng, X., 2010b. Core and sub-channel analysis of SCWR with mixed spectrum core. Annals of Nuclear Energy 37, 1674–1682.

Liu, X.J., Cheng, X., 2010c. Coupled thermal-hydraulics and neutron-physics analysis of SCWR with mixed spectrum core. Progress in Nuclear Energy 52, 640–647.

Maráczy, C., Hegyi, Gy., et al., 2011. HPLWR equilibrium core design with the KARATE-code system. Progress in Nuclear Energy 53, 267–277.

Marleau, G., Hébert, A., Roy, R., 2010. A User's Guide for DRAGON Version 4. Institut de génie nucléaire, Département de génie mécanique, École Polytechnique de Montsréal.

Oka, Y., Koshizuka, S., Ishiwatari, Y., et al., 2011. Super Light Water Reactors and Super Fast Reactors. Springer, Japan.

Schulenberg, T., Maráczy, C., et al., 2011. Assessment of the HPLWR thermal core design. In: ISSCWR-5, March 13–16, Vancouver, Canada.

Shan, J.Q., Zhang, B., et al., 2009. SCWR subchannel code ATHAS development and CANDU-SCWR analysis. Nuclear Engineering and Design 239, 1979–1987.

Yamaji, A., Oka, Y., Koshizuka, S., 2005a. Three-dimensional core design of high temperature supercritical-pressure light water reactor with neutronic and thermal-hydraulic coupling. Journal of Nuclear Science and Technology 42 (1), 8–19.

Yamaji, A., Kamei, K., Oka, Y., Koshizuka, S., 2005b. Improved core design of the high temperature supercritical-pressure light water reactor. Annals of Nuclear Energy 32, 651–670.

Yang, P., Cao, L.Z., Wu, H.C., et al., 2011. Core design study on CANDU-SCWR with 3D neutronic/thermal-hydraulics coupling. Nuclear Engineering and Design 241, 4714–4719.